

Raman spectra of $(\text{Bi,Pb})_2\text{Sr}_2\text{CaCu}_2\text{O}_{8+y}$ single crystals and the role of lead substitution

J. Sapiel, J. Schneck, J. F. Scott,* J. C. Tolédano, L. Pierre, J. Chavignon, and C. Daguet
Centre National d'Etudes des Télécommunications, 196 avenue Henri Ravéra, 92220 Bagneux, France

J. P. Chaminade

Laboratoire de Chimie du Solide du CNRS, 33405 Talence CEDEX, France

H. Boyer

Instrument S. A. Jobin et Yvon Division, Boîte Postale 118 Longjumeau CEDEX, France

(Received 20 August 1990)

We report the Raman spectra of chemically characterized $(\text{Bi}_{2-x}\text{Pb}_x)\text{Sr}_2\text{CaCu}_2\text{O}_{8+y}$ single crystals for $0 < x < 0.4$. Significant modifications of the spectra, becoming more pronounced with increasing x , are noted with respect to the lead-free crystals in the ranges of the 117-cm^{-1} , $(460\text{--}530)\text{-cm}^{-1}$, and $(630\text{--}650)\text{-cm}^{-1}$ lines. The interpretation of these modifications provides an important confirmation of recent speculations concerning the lattice dynamics of this family of superconductors and the role of lead in modifying their structure and their microstructure.

Few results relative to the Raman spectra of lead-substituted samples of the Bi-Sr-Ca-Cu-O superconductors have been published recently.^{1,2} Moreover, up to now, the specific influence of the lead substitution on these spectra has neither been analyzed in detail nor interpreted. This is partly due to the fact that information on the lead content of the phases considered was lacking. It has been suggested that the lead ions Pb^{2+} substitute mainly for the Bi^{3+} ions in the structure. This statement relies on few experimental facts. It stems, for instance, from the results of local chemical electron microanalysis,³ at a scale of $\sim 10 \text{ \AA}$. Structural fits of powder x-ray data indicate, on the other hand, that 50% of the lead is in Bi sites while 35% occupies Sr sites.⁴ Studies of the evolution of the incommensurate modulation as a function of the lead doping⁵ provide, at present, the most convincing, though less direct, evidence of the predominant location of lead on bismuth sites. In contrast with this set of evidence, a recent power neutron study has assigned the location of most Pb ions at calcium sites.⁶

It would be particularly desirable to lift this uncertainty and determine the influence on the Raman spectra of the introduction of lead in these structures, considering, on one hand, the absence of other accurate structural data for the lead-substituted phases, and on the other hand, the practical importance of lead substitution in promoting, within this family of superconductors, the phase possessing the highest critical temperature.

In this paper, we report Raman scattering results, in a $z(xx)z(\alpha_{xx})$ or a $z(yy)z(\alpha_{yy})$ scattering configuration, for five single crystals of the so-called 2:2:1:2 phase whose layered structure involves two CuO_2 planes per elementary structural unit. These crystals have compositions close to $\text{Bi}_{2-x}\text{Pb}_x\text{Sr}_2\text{CaCu}_2\text{O}_{8+y}$, and correspond to $x = 0, 0.1, 0.13, 0.25,$ and 0.4 . Significant modifications with respect to the spectra of lead-free crystals are noted. They are interpreted on the dual basis (a) of the lattice-dynamical model developed by Prade *et al.*⁷ for the lead-free crystals, and (b) of the structural and microstructural role recently assigned to the lead substitution.⁸ The consistency

of this interpretation provides an important experimental test in favor of the preceding considerations [(a) and (b)].

Single-crystalline platelets, perpendicular to the c axis, and of lateral sizes ranging from a fraction of a millimeter to a few millimeters were elaborated by slowly cooling melts of composition $(\text{Bi}_{2-x}\text{Pb}_x\text{Sr}_2\text{CaCu}_2\text{O}_{8-x/2} + 7\text{CuO})$ with $0 < x < 0.8$. Chemical analysis was effected by means of a micrometer-size electron microprobe. It showed uniform composition across the surface of the crystals, but a significant loss of lead with respect to the initial composition, the value $x = 0.4$ corresponding to the maximum achievable amount compatible with lead solubility, in agreement with many previous observations.⁸

The Raman spectra were obtained at room temperature using either a Raman microprobe (for the smallest crystals) or a standard Raman configuration. In both cases we used a setup and a procedure previously described.¹ Though we explored apparently untwinned regions of the crystals, no significant difference in the results was found between the α_{xx} and α_{yy} scattering configurations.

In sintered ceramics, the Raman spectra are sometimes misleading, due to the presence of parasitic phases. Our samples are single crystals in which this presence is less probable, and in which none could be detected through the use of x-ray diffraction. Moreover, the uniformity of the Raman spectra was checked by scanning the Raman microprobe across the surface of the samples. Hence, the lines detected in this study are likely to correspond to the intrinsic spectrum of the 2:2:1:2 phase (except for the effects of the intergrowth discussed below).

The spectrum, in the $50\text{--}700 \text{ cm}^{-1}$ range, of crystals corresponding to $x = 0.1$ is reproduced in Fig. 1. It differs little from that of the reference lead-free crystals. On the other hand, Figs. 2 and 3 display, respectively, in the range $50\text{--}150$ and $400\text{--}700 \text{ cm}^{-1}$, the evolution, as a function of the lead content, of the spectra of the crystals.

Four prominent features arising in the lead-doped crystals, and becoming more pronounced with increasing lead content, can be noted in these spectra. (i) The weak

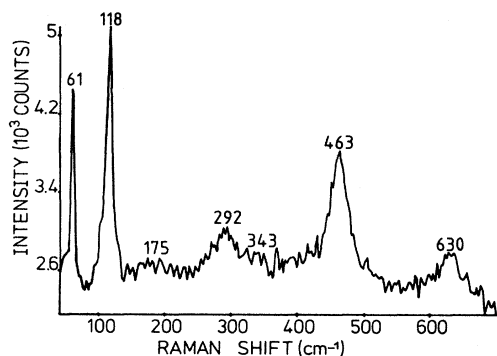


FIG. 1. Raman spectrum in a $z(xx)z$ scattering configuration of a crystal of composition $\text{Bi}_{1.9}\text{Pb}_{0.1}\text{Sr}_{1.75}\text{Ca}_{1.16}\text{Cu}_{1.96}\text{O}_y$ ($\lambda = 5145 \text{ \AA}$, resolution 3 cm^{-1}). This spectrum only differs from that of a lead-free crystal by the absence of a small line at 650 cm^{-1} .

α_{xx}, α_{yy} line at $\sim 650 \text{ cm}^{-1}$ disappears, even for small lead doping. (ii) The line at $\sim 630 \text{ cm}^{-1}$ increases in intensity and becomes narrower with increasing lead content. (iii) The single line at 463 cm^{-1} is replaced by a wide band extending from 450 to 570 cm^{-1} . In this band, two peaks can still be distinguished: the initial one at $\sim 460 \text{ cm}^{-1}$ and one at $\sim 530 \text{ cm}^{-1}$. (iv) The line at $\sim 117 \text{ cm}^{-1}$ is shifted towards lower frequencies. For $x=0.4$ the measured shift is $\sim 8.5 \text{ cm}^{-1}$. Though the

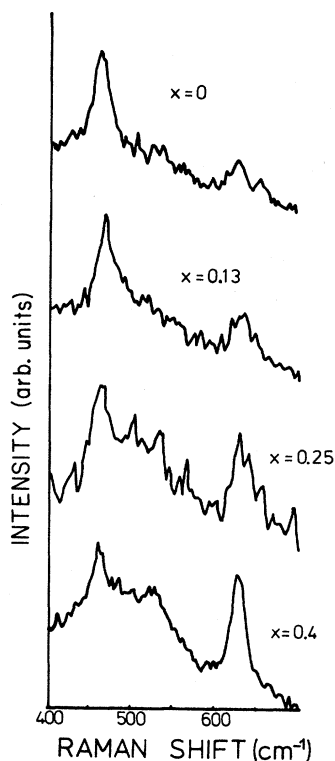


FIG. 2. High-frequency modes of lead-doped single crystals as a function of the lead content x in $\text{Bi}_{2-x}\text{Pb}_x\text{Sr}_2\text{CaCu}_2\text{O}_{8+y}$, obtained with a Raman-microprobe setup (spatial resolution $1 \mu\text{m}^2$, $\lambda = 5145$, or 4880 \AA).

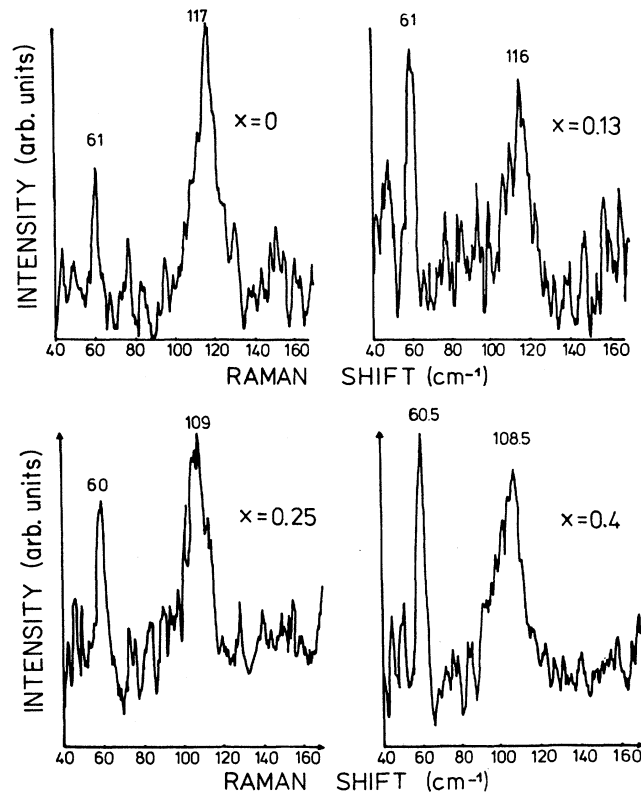


FIG. 3. Low-frequency modes of lead-doped single crystals as a function of the lead content x , obtained in a Raman-microprobe setup with a multichannel analyzer. ($\lambda = 5145 \text{ \AA}$, frequency resolution 6 cm^{-1}). Note the constancy of the 61 cm^{-1} mode and the downward shift of the 117 cm^{-1} one.

available data are insufficient to be sure, it is likely that this shift is continuous since the structural parameters (lattice constants, modulation wavelength) have been found to vary smoothly in the same samples.⁵

An interpretation of these results requires recalling the assignments, in terms of collective atomic motions, of the Raman lines of the lead-free crystals of the 2:2:1:2 phase. A model of the lattice dynamics of the 2:2:1:2 phase has been developed by Prade *et al.*⁷ in the framework of a simplified picture of the crystal structure. This model considers a structure with tetragonal symmetry $I4/mmm$, having a primitive unit cell containing a single formula unit $\text{Bi}_2\text{Sr}_2\text{CaCu}_2\text{O}_8$. This structure is constituted by a stacking, along the c axis, of slabs having a thickness of $\sim 12.5 \text{ \AA}$. Each slab consists of a pair of BiO planes enclosing a layered structure involving the remaining atoms (Sr, Ca, Cu, O). Hence, two adjacent slabs have their BiO planes facing each other, with an oxygen atom in one plane facing a bismuth atom in the other plane.

For this simplified structure, the calculations of Prade *et al.*⁷ yield the six A_{1g} modes, at $87, 164, 182, 387, 493,$ and 517 cm^{-1} . They also locate the B_{1g} mode at 347 cm^{-1} . These are the modes which one expects to observe in the scattering configuration used in this work.

The actual structure differs from the simplified one in a number of aspects: incommensurate modulation of the

atomic positions along the [010] direction, twofold superstructure along the [101] direction defining a primitive unit cell containing two formula units, and orthorhombic distortion. Some of these features involve large atomic displacements, and they could therefore modify significantly the lattice dynamics of the actual crystals with respect to the one calculated by Prade *et al.*⁷ Nevertheless, the latter calculations appear as a useful basis of interpretation: it is possible to establish a consistent correspondence between the lines experimentally assigned to the subcell, and the calculated ones.

On the basis of recent experimental results^{1,9-12} (including the present ones) the six A_{1g} modes of the subcell are found at $\sim 61, 117, 175, 343, 463$ and 650 cm^{-1} , while the B_{1g} mode is found at $\sim 292 \text{ cm}^{-1}$. Note that the sums of the calculated and the observed frequencies of the A_{1g} modes coincide within 1%, as expected if the distortion of the reference structure is not too large.¹³ Besides, the collective atomic motions assigned to each line in the framework of the theoretical model are consistent with various partial assignments based on experimental grounds.⁹⁻¹²

Let us examine, in the light of the preceding correspondence between calculated modes and experimental lines, the interpretation of the aforementioned observations (i)–(iv) relative to the influence of lead substitution. The basis of this interpretation resides in two key effects of the doping by lead.

One effect consists of a drastic reduction of an intercalation type of intergrowth between the dominant 2:2:1:2 phase and other parasitic phases belonging to the same structural family. In lead-free crystals, the occurrence of such an intergrowth seems to be the most frequently encountered situation:¹⁴ slabs of different thickness (corresponding to different superconducting phases having different numbers of CuO₂ planes within a slab) are stacked upon each other along the c axis, with only short-range order along c for each phase (a few tens of angstroms typically as shown by high-resolution electron microscopy¹⁴).

By contrast, in the lead-doped samples, there is effectively an absence of intergrowth at such a small scale, as pointed out by several authors.¹⁵ This different behavior is already observed for small levels of doping.

The other important effect is a modification of the binding scheme between adjacent slabs of the structure. On the basis of a number of experimental observations⁸ and consistent with the idea that lead predominantly substitutes for bismuth, it has been suggested recently⁸ that the doping by lead has the effect of strongly binding adjacent slabs in the structure, while these slabs are only loosely bonded in the absence of lead. Due to the valency change implied, the substitution of bismuth by lead probably induces covalent bonds between BiO planes while no such bonds exist in the prototype, lead-free structure, the bismuth atoms being covalently bonded only within the BiO plane and to the neighboring SrO plane.¹⁶

Let us first analyze the observations (i) and (ii) relative to the 650- and 630-cm⁻¹ lines, and show that the changes induced in these two lines by the lead doping are two converse effects of the suppression of the intergrowth between the dominant 2:2:1:2 phase and the so-called

2:2:0:1 phase which has a single CuO₂ plane per elementary structural unit.

For a reason which is not clear at present, in the lead-free samples of the 2:2:1:2 phase, the 650-cm⁻¹ A_{1g} mode is observed as the most intense Raman line in the $x(zz)x$ or $y(zz)y$ (α_{zz}) scattering configuration while in the α_{xx} or α_{yy} scattering configuration, its intensity is small, and varies greatly from sample to sample.⁹⁻¹² One also observes, in the α_{xx} or α_{yy} geometry, another A_{1g} line at 630 cm⁻¹. On the other hand, the Raman spectrum of the 2:2:0:1 phase¹² contains an A_{1g} line at 650 cm⁻¹, which is clearly observed in the α_{xx} or α_{yy} scattering configuration, and which probably constitutes the counterpart, for this phase, of the 630-cm⁻¹ line of the 2:2:1:2 phase.

Considering the general occurrence of intergrowth defects in the lead-free samples of the 2:2:1:2 phase, we can assume that, in this spectral range, the intrinsic A_{1g} line of the 2:2:1:2 phase, which must correspond with the lattice modes of Prade's model, is the 650-cm⁻¹ intense line detected in the α_{zz} scattering configuration. The one detected with variable magnitude in the α_{xx} or α_{yy} scattering configuration must be assigned to the 2:2:0:1 phase present as an intergrowth defect in variable proportions.

The vanishing of this line in the lead-doped crystals corresponds to the disappearance of the 2:2:0:1 phase, through elimination of the intergrowth. Note that, aside from the 650-cm⁻¹ line, the remaining α_{xx} spectrum of the 2:2:0:1 phase (above 100 cm⁻¹) resembles closely that of the 2:2:1:2 phase. It is, therefore, not surprising to detect the presence of this parasitic phase through the sole 650-cm⁻¹ line.

The 630-cm⁻¹ line, though clearly identified as an A_{1g} line, cannot belong to the set of A_{1g} modes of the subcell considered by Prade *et al.*⁷ Indeed, in this spectral range, the A_{1g} line is clearly the intense α_{zz} 650-cm⁻¹ line already discussed. Necessarily, the 630-cm⁻¹ line is an additional intrinsic A_{1g} mode, arising from the fact that the actual structure has a larger unit cell than the one considered by Prade. This is in agreement with available crystallographic data which show that there is, in particular, a doubling of the translational periodicity, with respect to the subcell, along the c direction. Given its proximity with the 650-cm⁻¹ line, the 630-cm⁻¹ line is likely to be a Brillouin-zone boundary mode (in the c direction) referred to the subcell, folded to the zone center of the enlarged cell, and belonging to the same, relatively flat, optic branch as the 650-cm⁻¹ mode. The Raman activation of this mode by the Brillouin-zone folding will be very perturbed by the occurrence of an intercalation type of intergrowth between the 2:2:1:2 phase and parasitic phases, which affects the long-range order of the translational periodicity along c . We can, therefore, expect that the 630-cm⁻¹ folded line will be weakened and widened in lead-free samples. Conversely, we can understand that the suppression of the intergrowth by the lead doping restores the intrinsic behavior, i.e., a narrower and more intense line at this frequency, in agreement with the present observations. The fact that, in the lead-doped crystals, this folded line has an intensity comparable to that of ordinary lines of the spectrum (e.g., the 117-cm⁻¹ line) is not surprising, since the structural distortions leading to

its Raman activation are large.

Let us now consider the modifications (iii) of the spectrum in the neighborhood of the 463-cm^{-1} line. Again, we interpret this modification by combining the results of Prade's lattice-dynamical model and the structural modifications assigned to the lead doping. This line is assigned to a collective motion, parallel to the c axis, of oxygen atoms surrounding the bismuth atoms. These atoms, located in the SrO and BiO planes, move together in phase. Note that the distance between a bismuth atom and an oxygen atom located in BiO planes of adjacent slabs is oscillating. This relative oscillation will be very sensitive to the strengthening of the binding force between slabs, which is induced, as mentioned above, by the introduction of lead in the structure. On this basis, we can expect, on the one hand, an important upward shift of the characteristic frequency of the 463-cm^{-1} mode (the mass of lead being almost identical to that of bismuth, and the restoring force of the motion being significantly larger), and, on the other hand, a certain distribution of frequencies related to the fact that 20% of lead, at most, is randomly substituted within the structure and that a variety of binding forces will be encountered depending of the region of the sample. The observations described in (iii) agree with this qualitative description: the single-line spectrum of the lead-free crystal is extended, in the lead-doped crystals, by a band at higher frequencies, which gains importance with increased lead doping. Due to the fact that our samples are single crystals, this phonon band is likely to be intrinsic to the investigated crystal compositions. It is worth pointing out that, in sintered ceramics elaborated beyond the limit of lead solubility, a Raman line (535 cm^{-1}) has been recently found¹⁷ in the same frequency range as the band discussed here, and has been assigned to a parasitic phase.

Finally, let us consider the downward frequency shift of

the 117-cm^{-1} mode. Its frequency being intermediate between that of the 87- and 164-cm^{-1} modes calculated by Prade *et al.*,⁷ its eigenvector is likely to be an admixture of the eigenvectors of the last two modes. Hence, it is associated predominantly with a collective motion of strontium and copper atoms within the subcell.⁷ This motion will not be affected significantly either by the modifications taking place in the intergrowth or in the binding scheme of the slabs, since both effects arise at the borderline between BiO planes. Though a variety of possible causes may be at the origin of this shift, a simple explanation consists of assigning it to a change of mass of the constituents. This would be consistent with certain x-ray data⁴ indicating that strontium is partly substituted by lead. Using the proportions indicated in Ref. 4 (35% of the Pb ions in Sr sites) and assuming, for the sake of simplicity, that the mass of the considered mode is that of strontium, we find that the downward frequency shift of this mode should be $\sim 5\%$, in good qualitative agreement with the observed $\sim 7\%$.

In conclusion, we have shown how the two key roles of lead, i.e., modifications of the intergrowth habit and of the binding scheme between slabs, has allowed one to account satisfactorily for the spectra of the lead-doped $\text{Bi}_2\text{Sr}_2\text{CaCu}_2\text{O}_8$. The present experimental results appear consistent with the available lattice dynamical model, and the assumption that lead substitutes for predominantly bismuth and strontium secondarily. These results seem to rule out the predominant location of lead on calcium sites. We have also clarified the assignments of the various closely spaced lines which are observed in the $(630\text{--}650)\text{-cm}^{-1}$ range. An assignment remains to be performed in the low-frequency range of the spectrum (below 50 cm^{-1}) where we have recently observed several lines in the lead-free and the lead-substituted samples.

*Permanent address: Department of Physics University of Colorado, Boulder, CO 80309-0390.

¹J. Sapriel, L. Pierre, D. Morin, J. C. Tolédano, J. Schneck, H. Savary, J. Chavignon, J. Primot, C. Daguet, and J. Etrillard, *Phys. Rev. B* **39**, 339 (1989).

²T. Suzuki, K. Hotta, Y. Koiwe, and H. Hirose, in *Proceedings of the First International Symposium on Superconductivity 1988, NAGOYA* (Springer-Verlag, Tokyo, 1989).

³H. Nobumasa, T. Arima, K. Shimizu, Y. Otsuka, Y. Murata, and T. Kawai, *Jpn. J. Appl. Phys.* **28**, L57 (1989).

⁴N. Kijima, H. Endo, J. Tshuchiya, A. Sumiyama, M. Mizuno, and Y. Oguri, *Jpn. J. Appl. Phys.* **28**, L787 (1989).

⁵L. Pierre, J. Schneck, D. Morin, J. C. Tolédano, J. Primot, C. Daguet, and H. Savary, *Ferroelectrics* **105**, 81 (1990).

⁶A. Sequeira, J. V. Yakhmi, R. M. Iyer, H. Rajagopal, and P. V. P. S. S. Sastry, *Physica C* **167**, 291 (1990).

⁷J. Prade, A. D. Kulkarni, F. W. de Wette, U. Schröder, and W. Kress, *Phys. Rev. B* **39**, 2771 (1989).

⁸L. Pierre, J. Schneck, D. Morin, J. C. Tolédano, J. Primot, C. Daguet, and H. Savary, *J. Appl. Phys.* (to be published); J. C. Tolédano, A. Litzler, J. Primot, J. Schneck, L. Pierre, D. Morin, and C. Daguet, *Phys. Rev. B* **42**, 436 (1990).

⁹M. Cardona, C. Thomsen, R. Liu, H. G. Von Schnering, M. Hartweg, Y. F. Yan, and Z. X. Zhao, *Solid State Commun.* **66**, 1225 (1988).

¹⁰F. Slakey, M. V. Klein, E. D. Bukovski, and D. M. Ginzberg, *Phys. Rev. B* **41**, 2109 (1990).

¹¹M. Boekholt, A. Erle, P. C. Splittberger-Hünnekes, and G. Guntherodt, *Solid State Commun.* **74**, 1107 (1990).

¹²V. N. Denisov, B. N. Marvin, V. B. Podobedov, I. V. Aleksandrov, A. B. Bykov, A. F. Gontcharov, O. K. Melnikov, and N. J. Ronanda, *Solid State Commun.* **70**, 885 (1989).

¹³The trace of the dynamical matrix is approximately preserved: see for instance D. C. Wallace, *Thermodynamics of Crystals* (Wiley, New York, 1972), p. 177.

¹⁴Y. Matsui, Y. Takegawa, H. Nozaki, A. Umezono, M. Takayama, and S. Hirochi, *Jpn. J. Appl. Phys.* **27**, L1241 (1988).

¹⁵Y. Hirotsu, O. Tomioka, N. Yamamoto, Y. Nakamura, S. Nagakura, Y. Iwai, and M. Takata, *Jpn. J. Appl. Phys.* **28**, L1783 (1989).

¹⁶Y. Le Page, W. R. Mc Kinnon, J. M. Tarascon, and P. Barboux, *Phys. Rev. B* **40**, 6810 (1989).

¹⁷L. A. Farrow, R. Ramesh, J. M. Tarascon, and S. M. Green, in *SPIE Conference Proceedings No. 1331* (to be published).